

Indicator Functions for Shape Reconstruction Related to the Linear Sampling Method

T. Arens* A. Lechleiter†

November 24, 2014

Abstract

We provide exact shape reconstruction formulas in the spirit of the Linear Sampling method for a class of inverse problems in shape determination in the context of time-independent partial differential equations. To this end, we prove a general theorem how, and under which assumptions, domain characterizations based on the range of the square root of an operator transform into domain characterizations based on the operator itself. To show the flexibility of this general theory we apply this general principle to a variety of shape determination problems in inverse acoustic and electromagnetic scattering theory and inverse elliptic boundary value problems. Further, we also establish a regularization strategy for noisy measurement operators.

1 Introduction

We consider inverse shape determination problems for elliptic partial differential equations. Examples include for instance inverse scattering problems where one seeks to find the shape of a scatterer from measured far field data of acoustic or electromagnetic waves, or inverse elliptic boundary value problems, where the most prominent application is electrical impedance tomography.

To tackle these problems we apply a version of the Linear Sampling method first introduced in [10, 12] for shape identification problems in scattering theory. Let us briefly recall that the method is based on the far field operator F , since it tries to determine the shape of the scatterer via approximate solutions g_z to the far field equation

$$(Fg_z)(\hat{x}) = e^{-ik\hat{x}\cdot z}, \quad \hat{x} \in \mathbb{S}^{d-1} = \{x \in \mathbb{R}^d, |x| = 1\}$$

for sampling points $z \in \mathbb{R}^d$ from a grid covering a domain of interest. Here k denotes the wave number. Since the far field operator is compact, a regularization scheme must be applied to this linear problem: The typical choice is Tikhonov regularization,

$$g_z^\varepsilon = (\varepsilon I + F^*F)^{-1}F^* \mathbf{e}[z] \quad \text{where } \mathbf{e}[z](\hat{x}) := e^{-ik\hat{x}\cdot z}, \quad (1)$$

combined with a discrepancy principle to choose the value of the regularization parameter $\varepsilon > 0$. The shape of the scatterer is then found as the set of those points z where the norm

*Karlsruher Institut für Technologie, Department of Mathematics, Karlsruhe, Germany

†Center for Industrial Mathematics, University of Bremen, Bremen, Germany

of g_z^ε is above a certain cut-off value that enters the algorithm as a parameter. Note that the theory on this method remains somewhat incomplete as the theoretical backbone of the method is a theorem claiming that for points inside the scattering object there exists an approximate solution to the far field equation that blows up as the regularization parameter tends to zero. However, there is no guarantee that the Tikhonov regularization g_z^ε from (1) behaves in the same way. However, it was already proposed in [10] to use the alternative indicator function

$$z \mapsto \left| \int_{\mathbb{S}^{d-1}} e^{ik \cdot \theta \cdot z} g_z^\varepsilon(\theta) ds(\theta) \right|, \quad z \in \mathbb{R}^d. \quad (2)$$

In [3, 4] we showed that this variant of the Linear Sampling method yields indeed a mathematically sound way to characterize a Dirichlet scattering object in \mathbb{R}^3 since, roughly speaking, the technique is equivalent to the Factorization method, first developed in [19].

For other scattering problems, such results have not yet been published, despite they certainly are of interest in, e.g., electromagnetic inverse scattering problems (see, e.g., the discussion in the end of Chapter 3.3 of [6]).

The above-described gap in the theory on the Linear Sampling method motivated several approaches to set the method onto mathematically sounder feet and we want to briefly discuss a couple of them. The three approaches we indicate all go into completely different directions than the present work: The paper [14] validates the Linear Sampling method as a shape identification technique in the low-frequency limit, whereas [16] considers the method in the context of theoretical results on Tikhonov regularization with inconsistent exact right-hand sides. Finally, [1] analyzes the Linear Sampling method via the flow strips of the Poynting vector associated to the scattered field.

In this paper, we prove that a generalization of (2) applied to a general inverse shape identification problem for a time-independent partial differential equation analogously yields a mathematically rigorous way of determining the shape of an obstacle. The main assumption of this generalization is that, roughly speaking, the Factorization method works when applied to the same problem. We give detailed examples for suitable shape identification problems in obstacle and electromagnetic medium scattering as well as in impedance tomography, and further note without going into details several problems the technique can also be applied to (e.g., linear elasticity, low-frequency electromagnetics and time-independent Stokes flows).

Going beyond the scope of [4], we also show that the alternative formulation of the Linear Sampling method does not only work when Tikhonov regularization is used. Indeed, arbitrary linear regularization schemes defined using regularizing filters can be employed to achieve the same theoretical properties for the resulting method.

Additionally, we provide a regularization theory for the presented alternative formulation of the Linear Sampling method that is able to cope with noisy measurements. In the context of sampling methods this generally means to deal with noisy measurement operators that are, roughly speaking, inverted on exact right-hand sides. The shape reconstruction criterion is shown to converge point wise as the noise level tends to zero if the regularization parameter of the scheme respects several bounds that are determined, roughly speaking, by the noise level.

Let us finally note that the alternative formulation of the Linear Sampling method for scalar, acoustic scattering problems is based on Herglotz wave functions. The analogous reformulation for electromagnetic problems is naturally based on dot products of curls of electromagnetic Herglotz wave functions with polarization vectors. The generalization to inverse elliptic problems as, e.g., impedance tomography relies on dot products of gradients of layer potentials for the corresponding Green's function with similar polarization vectors.

Let us briefly outline the structure of this paper: In the next Section 2 we present three inverse shape identification problems and, using suitable notation for later purposes, already indicate how the factorization method can be applied to them. We moreover show several crucial properties of the operators in the corresponding factorizations that will be required for an application of our general theory developed in Section 3. In Section 4 we provide regularization theory for the alternative Linear Sampling method for general linear regularization schemes. Section 5 contains numerical examples for inverse electromagnetic scattering from penetrable dielectrics.

Notation: We consider partial differential equations in a subset Ω of the d -dimensional Euclidean space \mathbb{R}^d , $d \geq 2$. Considering either scalar- or vector-valued problems, we rely on real- or complex-valued functions or distributions with $m \in \mathbb{N}$ components. These distributions typically will belong to Hilbert spaces $H^s(U, \mathbb{R}^m)$ or $H^s(U, \mathbb{C}^m)$ for some set $U \subset \mathbb{R}^d$ and some regularity parameter $s \in \mathbb{R}$. The symbols x, y and \hat{x} denote points in \mathbb{R}^d and unit vectors in $\mathbb{S}^{d-1} = \{y \in \mathbb{R}^d, |y| = 1\}$, respectively. The symbol D is reserved for bounded Lipschitz domains in \mathbb{R}^d that play the role of scattering objects in the different settings under investigation; the exterior unit normal field to ∂D is denoted by ν . The ball of radius $R > 0$ around a point $x \in \mathbb{R}^d$ is $B_R(x) = \{y \in \mathbb{R}^d, |x - y| < R\}$.

2 Applications of the Factorization Method

In this section we present three basic settings where the Factorization method can be applied to rigorously characterize inclusions in a background medium from the knowledge of solutions to partial differential equations involving these inclusions. In detail, we consider acoustic and electromagnetic scattering problems involving impenetrable and penetrable scatterers, respectively, as well as a shape identification problem in impedance tomography.

2.1 Scattering of Acoustic Waves from an Impenetrable Obstacle

The Helmholtz equation with wave number $k > 0$ models scattering of linear time-harmonic acoustic waves in the exterior of a bounded, impenetrable obstacle $D \subset \mathbb{R}^d$, $d = 2$ or 3 ,

$$\Delta u + k^2 u = 0 \quad \text{in } \mathbb{R}^d \setminus \overline{D}. \quad (3)$$

We assume that D is a bounded Lipschitz domain and consider, for $\tau \in L^\infty(\partial D, \mathbb{R})$, one of the following boundary conditions for the total wave field $u : \mathbb{R}^d \setminus \overline{D} \rightarrow \mathbb{C}$ on ∂D ,

$$\mathcal{B}(u) := u|_{\partial D} = 0 \quad \text{for a sound-soft obstacle,} \quad (4)$$

$$\mathcal{B}(u) := \left[\frac{\partial u}{\partial \nu} + \tau u \right] \Big|_{\partial D} = 0 \quad \text{for a sound-hard } (\tau = 0) \text{ or a Robin } (\tau \neq 0) \text{ obstacle.} \quad (5)$$

The physically relevant impedance boundary condition requires $\text{Im } \tau > 0$ and cannot be considered here since it leads to a non-normal far field operator.

When an incident wave u^i solving the Helmholtz equation in \mathbb{R}^3 illuminates the obstacle D there arises a scattered field u^s such that the total field can be written as $u = u^i + u^s$ in $\mathbb{R}^d \setminus \overline{D}$. Moreover, u^s satisfies Sommerfeld's radiation condition, see [13, Section 2.2]. Under this condition,

$$u^s(x) = \gamma_d \frac{e^{ik|x|}}{|x|^{(d-1)/2}} u^\infty(\hat{x}) + \mathcal{O}\left(\frac{1}{|x|^{3/2}}\right) \quad \text{as } |x| \rightarrow \infty, \quad \text{uniformly in } \hat{x} = \frac{x}{|x|},$$

for the far field pattern $u^\infty : \mathbb{S}^{d-1} \rightarrow \mathbb{C}$ of u^s . Here $\gamma_3 = 1/(4\pi)$ while $\gamma_2 = \exp(i\pi/4)/\sqrt{8\pi k}$. Any solution to the Helmholtz equation that satisfies Sommerfeld's radiation condition is called a radiating solution. For the special setting of scattering of incident plane waves $x \mapsto \exp(ik\theta \cdot x)$ with direction $\theta \in \mathbb{S}^{d-1}$ we denote by $u^\infty(\cdot, \theta)$ the corresponding far field pattern. The inverse scattering problem we consider is to find the domain D given the far field patterns $u^\infty(\hat{x}, \theta)$ for all $\hat{x}, \theta \in \mathbb{S}^{d-1}$.

For all boundary conditions (4)–(5), the scattered field u^s is a radiating solution to (3) subject to the boundary condition $\mathcal{B}(u^s) = -\mathcal{B}(u^i)$ on ∂D . This scattering problem possesses a unique radiating solution $u^s \in H_{\text{loc}}^1(\mathbb{R}^d \setminus \overline{D})$ that is bounded in terms of $\mathcal{B}(u^i)$ [24, 26]: Setting $X = H^{1/2}(\partial D)$ in the sound-soft case and $X = H^{-1/2}(\partial D)$ both in the sound-hard or Robin case, it holds that for some $x_0 \in D$ and all $R > \text{diam}(D)$ there is $C = C(R)$ such that $\|u^s\|_{H^1(B_R(x_0) \setminus \overline{D})} \leq C(R)\|\mathcal{B}(u^i)\|_X$. Further, the far field operator

$$F : L^2(\mathbb{S}^{d-1}) \rightarrow L^2(\mathbb{S}^{d-1}), \quad (Fg)(\hat{x}) = \int_{\mathbb{S}^{d-1}} u^\infty(\hat{x}, \theta) g(\theta) \, ds(\theta), \quad \hat{x} \in \mathbb{S}^{d-1}, \quad (6)$$

is linear and compact. Linearity of the scattering problem moreover implies that Fg is the far field pattern of the scattered field corresponding to an incident Herglotz wave function

$$v_g(x) = \int_{\mathbb{S}^{d-1}} e^{ikx \cdot \theta} g(\theta) \, ds(\theta), \quad x \in \mathbb{R}^d. \quad (7)$$

For all three boundary conditions (4–5), the far field operator is normal (see, e.g., [21], [5, Th. 7.15]) and possesses a complete system of eigenvectors $\psi_j \in L^2(\mathbb{S}^{d-1})$ to eigenvalues $\lambda_j \in \mathbb{C}$ tending to zero as $j \rightarrow \infty$. In three dimensions λ_j lies on the circle with center $8\pi^2 i/k$ and radius $8\pi^2/k$; in two dimensions, the eigenvalues lie on the circle with center $\exp(3\pi i/4)\sqrt{2\pi/k}$ and radius $\sqrt{2\pi/k}$. Let us represent the eigenvalues λ_j as

$$\lambda_j = |\lambda_j| e^{i\beta} e^{i\delta_j}$$

with phases δ_j in the interval $[0, \pi]$ and a dimension-dependent phase shift $\beta = 0$ in three and $\beta = \pi/4$ in two dimensions. Independent of the boundary condition and the dimension d , the phases δ_j are even contained in a sub-interval of $[0, \pi]$ of length strictly smaller than π (see, e.g., [21] for the three-dimensional case and [11], [5, Th. 7.14] as well as [19, Section 5] for the two-dimensional case).

Let us now introduce the Herglotz operator $H : L^2(\mathbb{S}^{d-1}) \rightarrow X$ using v_g from (7) by

$$Hg = \mathcal{B}(v_g) \quad \text{on } \Gamma. \quad (8)$$

For the boundary conditions (4–5) it is obvious that H is bounded. If $G : X \rightarrow L^2(\mathbb{S}^{d-1})$ denotes the solution operator for the exterior scattering problem mapping the boundary datum in X to the far field of the solution u^s , then

$$F = GH. \quad (9)$$

The main result of the Factorization method applied to the above-introduced inverse scattering problem is the following: Depending on the choice of the boundary condition, assume that k^2 is not an interior Dirichlet-, Neumann- or Robin eigenvalue. Then the function

$$\theta \mapsto \mathbf{e}[z](\theta) := e^{-ik\theta \cdot z} \in L^2(\mathbb{S}^{d-1}), \quad \text{parametrized } z \in \mathbb{R}^d,$$

belongs to the range of $(F^*F)^{1/4}$ if and only if the point z belongs to the obstacle D . For details and proofs of this characterization we refer to Sections 1.4, 1.6 and 2.1–2.2 in [21].

2.2 Scattering of Electromagnetic Waves from a Non-Absorbing Medium

As a second example for an application of the Factorization method, we consider the scattering of electromagnetic waves by an inhomogeneous non-absorbing non-magnetic medium. Denote by ω the circular frequency, by ε_0 the electric permittivity and by μ_0 the magnetic permeability in vacuum. An electromagnetic-field propagating in \mathbb{R}^3 is a solution to the Maxwell system

$$\operatorname{curl} E - i\omega\mu_0 H = 0, \quad \operatorname{curl} H + i\omega\varepsilon_0 E = 0 \quad \text{in } \mathbb{R}^3. \quad (10)$$

We assume that the incident field (E^i, H^i) satisfying (10) is scattered by a bounded, non-conducting inhomogeneity characterized by a space-dependent permittivity ε . Then, the total field (E^t, H^t) is a solution to the Maxwell system (10) with ε_0 replaced by ε . The scattering problem is completed by requiring that the scattered field $E^s = E^t - E^i$, $H^s = H^t - H^i$ satisfies the well-known Silver-Müller radiation condition at infinity, see, e.g. [13, Section 6.2]. As a consequence, the scattered fields have an asymptotic behaviour similar to that of the acoustic scattered field u^s in Section 2.1. The far field patterns (E^∞, H^∞) are analytic functions on the unit sphere that satisfy $E^\infty(\hat{x}) \cdot \hat{x} = H^\infty(\hat{x}) \cdot \hat{x} = 0$ and $E^\infty(\hat{x}) = H^\infty(\hat{x}) \times \hat{x}$ for $\hat{x} \in \mathbb{S}^2$.

In what follows, we work with the magnetic field only. As presented in detail in [21, Section 5.2], the electric field can be eliminated from the Maxwell system. We obtain the equation

$$\operatorname{curl} [\varepsilon_r^{-1} \operatorname{curl} H^s] - k^2 H^s = \operatorname{curl} (qf) \quad \text{in } \mathbb{R}^3 \quad (11)$$

with $f = \operatorname{curl} H^i$, the wave number $k = \omega \sqrt{\varepsilon_0 \mu_0}$ and the relative permittivity $\varepsilon_r = \varepsilon / \varepsilon_0$. The contrast q is defined as $q = 1 - 1/\varepsilon_r$. We make the assumption that for some bounded Lipschitz domain $D \subseteq \mathbb{R}^3$ and some constants $c_1, c_2 > 0$, it holds that $\varepsilon_r \in L^\infty(D)$ with $\varepsilon_r \geq c_1$ and $\varepsilon_r - 1 \geq \pm c_2$ in D . Extending ε_r by 1 outside D , we have $\bar{D} = \operatorname{supp} q$. Lastly we will assume that (11) admits a unique radiating variational solution in $H_{\text{loc}}(\operatorname{curl}, \mathbb{R}^3)$ for all compactly supported $f \in L^2(\mathbb{R}^3, \mathbb{C}^3)$.

The inverse problem which can be solved by the Factorization method is to determine D from the knowledge of the far field patterns H^∞ for all plane incident waves

$$H^i(x) = p e^{ik\theta \cdot x}, \quad x \in \mathbb{R}^3, \quad (12)$$

where $p \in \mathbb{C}^3 \setminus \{0\}$ denotes the amplitude vector, $\theta \in \mathbb{S}^2$ the direction of incidence and we have $p \cdot \theta = 0$. To make plain the dependence on all parameters, we will write $H^i(x, \theta, p)$ for the incident plane wave with direction of incidence θ and amplitude p as well as $H^\infty(\hat{x}, \theta, p)$ for the far field of the corresponding scattered magnetic wave. Denoting by $L_t^2(\mathbb{S}^2)$ the space of all square-integrable tangential vector fields on the unit sphere, we introduce the *far field operator* $F : L_t^2(\mathbb{S}^2) \rightarrow L_t^2(\mathbb{S}^2)$ by

$$Fg(\hat{x}) = \int_{\mathbb{S}^2} H^\infty(\hat{x}, \theta, g(\theta)) \, ds(\theta), \quad g \in L_t^2(\mathbb{S}^2), \quad \hat{x} \in \mathbb{S}^2. \quad (13)$$

Note that H^∞ depends linearly on the polarization p of the incident plane wave and thus F is a linear operator. Further, F is compact and normal and thus possesses a complete orthonormal system of eigenfunctions. Moreover, the eigenvalues λ_j of F are all of the form $\lambda_j = |\lambda_j| e^{i\delta_j}$ with $0 \leq \delta_j < \pi$ for all $j \in \mathbb{N}$ and $\lim_{j \rightarrow \infty} \delta_j = 0$.

Introducing the Herglotz operator $H : L_t^2(\mathbb{S}^2) \rightarrow L^2(D, \mathbb{C}^3)$ by

$$Hg(x) = \operatorname{curl} \int_{\mathbb{S}^2} g(\theta) e^{ik\theta \cdot x} \, ds(\theta), \quad x \in D,$$

we see that Fg is the far field pattern of H^s for the incident field Hg . Thus, $F = GH$ holds for the solution operator $G : L^2(D, \mathbb{C}^3) \rightarrow L_t^2(\mathbb{S}^2, \cdot)$, mapping the right-hand side f in (11) to the far field pattern of the radiating solution to (11), compare [21, Theorem 5.10]. Even though the definition of H and G slightly differ from the presentation in [21, Chapter 5], neither the operator F nor the range of H^* change. In the case where k^2 is not a transmission eigenvalue (see Definition 5.8 in [21]), we conclude that D can be characterized as the set of points $z \in \mathbb{R}^3$ for which the function

$$\mathbf{e}[z, p](\hat{x}) = ik (\hat{x} \times p) e^{-ik\hat{x}\cdot z}, \quad p \in \mathbb{C}^3 \setminus \{0\}, \quad \hat{x} \in \mathbb{S}^2,$$

belongs to the range of $(F^*F)^{1/4}$. Note that we can rewrite the operator H by exchanging differentiation and integration to obtain

$$Hg(x) = \int_{\mathbb{S}^2} \text{curl} \left(g(\theta) e^{ik\theta\cdot x} \right) ds(\theta) = \int_{\mathbb{S}^2} ik (\theta \times g(\theta)) e^{ik\theta\cdot x} ds(\theta), \quad x \in D.$$

Extending the definition of Hg to all of \mathbb{R}^3 , it holds for $z \in \mathbb{R}^3$, $p \in \mathbb{C}^3$ and $g \in L_t^2(\mathbb{S}^2)$ that

$$\begin{aligned} p \cdot Hg(z) &= -ik \int_{\mathbb{S}^2} p \cdot (g(\theta) \times \theta) e^{ik\theta\cdot z} ds(\theta) \\ &= -ik \int_{\mathbb{S}^2} g(\theta) \cdot (\theta \times p) e^{ik\theta\cdot z} ds(\theta) = \langle g, \mathbf{e}[z, \bar{p}] \rangle_{L_t^2(\mathbb{S}^2)}. \end{aligned}$$

Remark 1. Analogously, one can apply the Factorization method to shape identification problems in low frequency electromagnetics within the magnetostatic or (with slight modifications) in the electrostatic limit, see [15], as well as in linear elasticity, see [2].

2.3 Electrical Impedance Tomography

Given a conductivity γ inside a body $\Omega \subseteq \mathbb{R}^d$ and a current density g on the boundary $\Gamma = \partial\Omega$, the electric potential u in Ω is a solution to the Neumann boundary value problem

$$\text{div}(\gamma \nabla u) = 0 \quad \text{in } \Omega, \quad \gamma \frac{\partial u}{\partial \nu} = g \quad \text{on } \Gamma. \quad (14)$$

We will assume throughout that the conductivity is real valued but possibly anisotropic, i.e.,

$$\begin{aligned} \gamma \in L_+^\infty(\Omega, \mathbb{R}^{d \times d}) := \{ \sigma \in L^\infty(\Omega, \mathbb{R}^{d \times d}) \text{ such that } \sigma(x)^\top = \sigma(x) \text{ and } \theta^\top \sigma(x) \theta \geq c \text{ for} \\ \text{some } c > 0, \text{ all } \theta \in \mathbb{S}^{d-1} \text{ and for almost all } x \in \Omega \}. \end{aligned}$$

Since all conductivities will be real-valued we can restrict ourselves to real-valued function spaces. Setting

$$L_\diamond^2(\Gamma) = \{ g \in L^2(\Gamma), \int_\Gamma g ds = 0 \} \quad \text{and} \quad H_\diamond^1(\Omega) = \{ u \in H^1(\Omega), \int_\Gamma u ds = 0 \},$$

Poincaré's inequality and Lax-Milgram's lemma imply that the variational formulation corresponding to (14)

$$\int_\Omega \gamma \nabla u \cdot \nabla v ds = \int_\Gamma gv ds \quad \text{for all } v \in H_\diamond^1(\Omega), \quad (15)$$

possesses a unique solution $u \in H_\diamond^1(\Omega)$.

In impedance tomography, one seeks to determine properties of the conductivity γ from boundary measurements of the electric potential on Γ . Mathematically, the boundary measurements of a voltage potential are encoded in the Neumann-to-Dirichlet operator $\Lambda : L^2_\diamond(\Gamma) \rightarrow L^2_\diamond(\Gamma)$. It maps $g \in L^2_\diamond(\Gamma)$ to $u|_\Gamma$, where $u \in H^1_\diamond(\Omega)$ is the unique solution to (15).

Assume now, additionally, that γ differs from a known background conductivity $\gamma_0 \in L^\infty_+(\Omega, \mathbb{R}^{d \times d})$ by a perturbation Q defined in a Lipschitz domain D such that $\overline{D} \subset \Omega$ and such that the support \overline{D} has a connected complement in \mathbb{R}^d ,

$$\gamma = \begin{cases} \gamma_0 + Q & \text{in } D, \\ \gamma_0 & \text{in } \Omega \setminus \overline{D}, \end{cases}$$

where $Q \in L^\infty_+(\Omega, \mathbb{R}^{d \times d})$ is again real-valued and symmetric positive definite. Denote by Λ_0 the corresponding Neumann-to-Dirichlet operator mapping g to $u_0|_\Gamma$, where $u_0 \in H^1_\diamond(\Omega)$ is the solution to (15) with γ replaced by γ_0 . Both Λ and Λ_0 are compact operators on $L^2_\diamond(\Gamma)$ due to the compactness of the trace operator from $H^1(\Omega)$ into $L^2(\Gamma)$. To state a factorization of the operator $\Lambda_0 - \Lambda$, we introduce two auxiliary operators. First, set

$$H : L^2_\diamond(\Gamma) \rightarrow L^2(D, \mathbb{R}^d), \quad g \mapsto \nabla u_0|_D \quad (16)$$

where $u_0 \in H^1_\diamond(\Omega)$ again solves (15) with $\gamma = \gamma_0$. Second, define

$$T : L^2(D, \mathbb{R}^d) \rightarrow L^2(D, \mathbb{R}^d) \quad f \mapsto Q(f - \nabla w),$$

where $w \in H^1_\diamond(\Omega)$ is a variational solution to

$$\int_\Omega \gamma \nabla w \cdot \nabla v \, dx = \int_\Omega (\nabla v)^\top Q f \, dx \quad \text{for all } v \in H^1_\diamond(\Omega).$$

Then $\Lambda_0 - \Lambda$ is compact, self-adjoint and positive on $L^2_\diamond(\Gamma)$, see [20, Th. 5.11], and

$$\Lambda_0 - \Lambda = H^* T H \quad \text{on } L^2_\diamond(\Gamma). \quad (17)$$

Since $\Lambda_0 - \Lambda$ is self-adjoint it possesses eigenvalues $\lambda_j \in \mathbb{R}$ and orthonormal eigenfunctions $\psi_j \in L^2_\diamond(\Gamma)$. Compactness and positivity of $\Lambda_0 - \Lambda$ show that $0 < \lambda_j \rightarrow 0$ as $j \rightarrow \infty$.

The operator H can alternatively be characterized using the Neumann function $\Phi_N(x, y)$ for the domain Ω , see [8, Th. 3.1] for Lipschitz domains and conductivities in $L^\infty_+(\Omega, \mathbb{R}^{d \times d})$ or [25] for domains and conductivities of class $C^{2,\alpha}$. Due to [8, Eq. (3.4)] the potential

$$u_0(x) = \int_\Gamma \Phi_N(x, y) g(y) \, dS(y), \quad x \in \Omega, \quad g \in L^2_\diamond(\Gamma), \quad (18)$$

is the unique variational solution in $H^1_\diamond(\Omega)$ to $\operatorname{div}(\gamma_0 \nabla u_0) = 0$ in Ω and $\gamma_0 \partial u_0 / \partial \nu = g$ on Γ . Hence, we find the following representation of the operator H from (16),

$$H g = \nabla u_0|_D = \left[\nabla_x \int_\Gamma \Phi_N(x, y) g(y) \, dS(y) \right] \Big|_D.$$

Given some polarization vector $p \in \mathbb{S}^{d-1}$, we set

$$\mathbf{e}[z, p](x) = p \cdot \nabla_z \Phi_N(x, z), \quad x \in \Gamma, \quad z \in \Omega.$$

The application of the Factorization method to the impedance tomography problem yields that $\mathbf{e}[z, p]$ belongs to the range of $(\Lambda_0 - \Lambda)^{1/2}$ if and only if $z \in D$ (see [20, Theorem 5.14]). Since $\Lambda_0 - \Lambda$ is self-adjoint, the square root $(\Lambda_0 - \Lambda)^{1/2} = [(\Lambda_0 - \Lambda)^*(\Lambda_0 - \Lambda)]^{1/4}$ can be defined via the eigendecomposition. Similarly to the Maxwell case, we obtain from the symmetry of the Neumann function with respect to its arguments that

$$p \cdot Hg(z) = p \cdot \nabla_z \int_{\Gamma} \Phi_N(z, y) g(y) ds(y) = \int_{\Gamma} p \cdot \nabla_z \Phi_N(y, z) g(y) ds(y) = \langle g, \mathbf{e}[z, p] \rangle.$$

Note that Chapter 5.4 in [20] in particular shows that $\mathbf{e}[z, p] \in L^2_{\diamond}(\Gamma)$ for $z \in \Omega$ and $p \in \mathbb{S}^{d-1}$.

Remark 2. *One can analogously apply the Factorization method to shape identification problems for the Stokes(-Brinkman) system in bounded domains, see [23].*

3 Domain Characterization

In this section, we will present a framework that allows to explain the relation between the Linear Sampling and the Factorization methods for all settings discussed in Section 2. The following definitions and assumptions are motivated by these applications and we expect that other problem classes fit into the same setting as well.

Subsequently, we will assume that $\Gamma \subset \mathbb{R}^d$ is some open or closed subset of the boundary of a Lipschitz domain; the relative interior of the $d - 1$ -dimensional surface Γ is always supposed to be non-empty. We assume further that F is a closed linear operator defined on a closed subspace Y_0 of some Hilbert space Y of \mathbb{C}^m -valued distributions on Γ , $m \in \mathbb{N}$. Moreover, Ω denotes a Lipschitz domain in \mathbb{R}^d .

Remark 3. *A slightly more general setting where F operates between dual spaces could also be employed at the expense of a more complicated notation.*

In the case of the scalar scattering problems in \mathbb{R}^d from Section 2.1 F corresponds to the far field operator from (6), $\Gamma := \mathbb{S}^{d-1}$, $Y = Y_0 = L^2(\mathbb{S}^{d-1})$, and $\Omega = \mathbb{R}^d$. For the Maxwell problem from Section 2.2, F corresponds to the far field operator from (13) and we have $\Gamma := \mathbb{S}^2$, $Y = L^2(\mathbb{S}^2, \mathbb{C}^3)$, $Y_0 = Y'_0 = L^2_t(\mathbb{S}^2)$, and $\Omega = \mathbb{R}^3$. Finally, for the impedance tomography problem from Section 2.3 F corresponds to the relative Neumann-to-Dirichlet operator $\Lambda_0 - \Lambda$ from (17), $\Omega \subset \mathbb{R}^d$, $\Gamma = \partial\Omega$ and $Y = L^2(\Gamma)$ as well as $Y_0 = L^2_{\diamond}(\Gamma)$. The next assumption links all these measurement operators to obstacles or inclusions inside Ω (compare Figure 1).

Assumption 4. *We assume that the linear operator F satisfies the following properties:*

- (A) *$F : Y_0 \rightarrow Y_0$ possesses an orthonormal eigensystem (λ_j, ψ_j) with eigenvalues $\lambda_j \neq 0$ and eigenvectors $\psi_j \in Y_0$, such that $Fg = \sum_{j \in \mathbb{N}} \lambda_j \langle g, \psi_j \rangle_Y \psi_j$ for all $g \in Y_0$. The phases δ_j of $\lambda_j / |\lambda_j| = \exp(i\delta_j)$ belong to some closed interval $J \subseteq \mathbb{R}$ with length $|J| < \pi$.*
- (B) *F possesses a factorization of the form $F = GH$ where H is a bounded linear operator from Y_0 into some Banach space X of \mathbb{C}^{ℓ} -valued distributions (with $\ell \in \mathbb{N}$) defined on a set $D \subset \Omega$ and $G : X \rightarrow Y_0$ is closed.*
- (C) *For all $x \in \Omega$ and $p \in \mathbb{S}^{\ell-1}$, it holds that $p \cdot (Hg)(x) = \langle g, \mathbf{e}[x, p] \rangle_Y$ for a family $\mathbf{e}[\cdot, \cdot] \in Y_0$ parametrized by $x \in \Omega$ and $p \in \mathbb{S}^{\ell-1}$.*

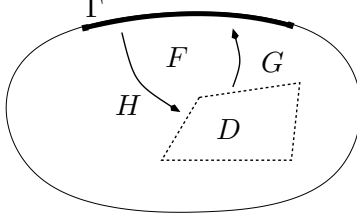


Figure 1: Sketch of the framework for shape identification using sampling methods.

(D) For any $p \in \mathbb{S}^{\ell-1}$, the function $\mathbf{e}[x, p] \in Y_0$ belongs to the range of $(F^*F)^{1/4} : Y_0 \rightarrow Y_0$ if and only if x belongs to $D \subset \Omega$.

From now on, we use the abbreviation

$$w_g : x \mapsto \langle g, \mathbf{e}[x, p] \rangle_Y, \quad x \in \Omega, \quad p \in \mathbb{S}^{\ell-1}, \quad (19)$$

for the operation mapping $g \in Y_0$ to the function $x \mapsto \langle g, \mathbf{e}[x, p] \rangle_Y$. Note that the polarization $p \in \mathbb{S}^{\ell-1}$ is in the sequel arbitrary, but fixed. This is the reason why we do not denote the dependency of w_g on this parameter explicitly.

Remark 5. (1) For the acoustic scattering problems from Section 2.1 w_g from (19) is a scalar Herglotz wave function, see (7). Indeed, $\ell = 1$ since the image space X of the operator H from (8) contains scalar distributions and hence $p \in \mathbb{S}^0$ is either plus or minus one. Without loss of generality we choose $p = 1$ and set $\mathbf{e}[x](\theta) := \mathbf{e}[x, 1](\theta) = \exp(-ik\theta \cdot x)$. Since $Y = L^2(\mathbb{S}^2)$,

$$w_g(x) = \langle g, \mathbf{e}[x] \rangle_Y = \int_{\mathbb{S}^{d-1}} e^{ik\theta \cdot x} g(\theta) \, ds(\theta) = v_g(x), \quad x \in \Omega = \mathbb{R}^d.$$

(2) The situation gets more complicated when considering the electromagnetic scattering problem from Section 2.2: We have $\ell = 3$ since $X = L^2(D, \mathbb{C}^3)$ is a space of vector-valued functions. The function w_g from (19) turns out to be the dot product of $p \in \mathbb{S}^{\ell-1} = \mathbb{S}^2$ with an electromagnetic Herglotz wave function with density $g \in Y_0 = L_t^2(\mathbb{S}^3)$,

$$\begin{aligned} w_g(x) = \langle g, \mathbf{e}[x, p] \rangle_Y &= \int_{\mathbb{S}^2} \overline{\mathbf{e}[x, p](\theta)} \cdot g(\theta) \, ds(\theta) = -ik \int_{\mathbb{S}^2} (\theta \times p) \cdot g(\theta) e^{ik\theta \cdot x} \, ds(\theta) \\ &= p \cdot \text{curl} \int_{\mathbb{S}^2} e^{ik\theta \cdot x} g(\theta) \, ds(\theta), \quad x \in \Omega = \mathbb{R}^3. \end{aligned}$$

(3) For the impedance tomography problem from Section 2.3 we have $\ell = d$ since $X = L^2(D)^d$. Hence, w_g from (19) is the directional derivative of a layer potential with density $g \in Y_0 = L_\diamond^2(\Gamma)$ in direction $p \in \mathbb{S}^{\ell-1} = \mathbb{S}^{d-1}$,

$$w_g(x) = \langle g, \mathbf{e}[x, p] \rangle_Y = \int_\Gamma p \cdot \nabla_z \Phi(x, y) g(y) \, dS(y) = \frac{\partial}{\partial p} \int_\Gamma \Phi(x, y) g(y) \, dS(y), \quad y \in \Omega \subset \mathbb{R}^d.$$

In the introduction we already mentioned the classical formulation of the Linear Sampling method for scalar inverse scattering problems, see (1). In the abstract framework detailed in Assumption 4, this method can be reformulated as follows: Use the contour lines of the function $z \mapsto \|g_z^\varepsilon\|$ where g_z^ε is an approximate solution to

$$Fg_z = \mathbf{e}[z, p] \quad \text{in } Y_0 \quad (20)$$

for parameters $z \in \Omega$ and $p \in \mathbb{S}^{\ell-1}$ to find the shape of the domain D . Using Tikhonov regularization to tackle the possibly ill-posed operator equation (20) together with the eigen-decomposition $(\lambda_j, \psi_j)_{j \in \mathbb{N}}$ of F yields approximate solutions

$$g_z^\varepsilon = (\varepsilon I + F^* F)^{-1} F^* \mathbf{e}[z, p] = \sum_{j \in \mathbb{N}} \frac{\overline{\lambda_j}}{|\lambda_j|^2 + \varepsilon} \langle \mathbf{e}[z, p], \psi_j \rangle_Y \psi_j, \quad z \in \mathbb{R}^d, \varepsilon > 0. \quad (21)$$

The regularization parameter ε has, again, to be chosen by a parameter choice, e.g., by the discrepancy principle. The claim of the Linear Sampling method is then that the contour lines of $z \mapsto \|g_z^\varepsilon\|_Y$ allow to detect the obstacle D since, for $z \in D$ there is a better approximation of $\mathbf{e}[z, p]$ in the range of F than for $z \notin D$. As mentioned in the introduction there is no rigorous proof for this statement. The basic motivation for the method is a result stating that there exists $g_{z, \varepsilon} \in Y_0$ with $\|F g_{z, \varepsilon} - \mathbf{e}[z, p]\| \leq \varepsilon$ such that for $z \in D$ and fixed $\varepsilon > 0$ it holds that $\|g_{z, \varepsilon}\| \rightarrow \infty$ as $z \rightarrow z^* \in \partial D$ while for $z \notin D$ it holds that $\|g_{z, \varepsilon}\| \rightarrow \infty$ as $\varepsilon \rightarrow 0$, see, e.g., [21, 5, 6]. The latter statement should be compared to point (D) of Assumption 4 that provides an exact characterization of D , replacing the range of F by the range of the square root $(F^* F)^{1/4}$. For all settings presented in Section 2 this point is precisely the statement of the Factorization method characterizing D from the measured data F .

Instead of restricting ourselves to Tikhonov regularization, we consider in the sequel any linear regularization scheme $R_\varepsilon : Y_0 \rightarrow Y_0$ defined via a regularizing filter function f_ε ,

$$R_\varepsilon g := \sum_{j \in \mathbb{N}} f_\varepsilon(|\lambda_j|^2) \langle F^* g, \psi_j \rangle_Y \psi_j = \sum_{j \in \mathbb{N}} f_\varepsilon(|\lambda_j|^2) \overline{\lambda_j} \langle g, \psi_j \rangle_Y \psi_j, \quad g \in Y_0. \quad (22)$$

The (standard) assumptions for the bounded and piecewise continuous filter $f_\varepsilon : (0, \infty) \rightarrow \mathbb{R}$ are

$$\lim_{\varepsilon \rightarrow 0} f_\varepsilon(\lambda) \rightarrow \frac{1}{\lambda} \quad \text{for all } \lambda > 0, \quad \lambda |f_\varepsilon(\lambda)| \leq C \quad \text{for all } \varepsilon \geq 0, \lambda > 0. \quad (23)$$

A classical example for a regularization scheme defined via a filter function that satisfies (23) is Tikhonov regularization. For this scheme, $f_\varepsilon(\lambda) = 1/(\lambda + \varepsilon)$ and we get as in (21),

$$g_z^\varepsilon = R_\varepsilon^{\text{Tik}} \mathbf{e}[z, p] = \sum_{j \in \mathbb{N}} \frac{\overline{\lambda_j}}{|\lambda_j|^2 + \varepsilon} \langle \mathbf{e}[z, p], \psi_j \rangle_Y \psi_j. \quad (24)$$

Another example is the singular value cut-off with

$$f_\varepsilon(\lambda) = \begin{cases} 1/\lambda, & |\lambda| \geq \varepsilon, \\ 0, & |\lambda| < \varepsilon. \end{cases}$$

Here,

$$g_z^\varepsilon = R_\varepsilon^{\text{svco}} \mathbf{e}[z, p] = \sum_{j: |\lambda_j| \leq \varepsilon} \frac{1}{\lambda_j} \langle \mathbf{e}[z, p], \psi_j \rangle_Y \psi_j. \quad (25)$$

Theorem 6. *Suppose that Assumption 4 holds, that $\{R_\varepsilon\}_{\varepsilon > 0}$ is a family of regularization schemes defined via a regularizing filter function, fix $p \in \mathbb{S}^{\ell-1}$, and define*

$$g_z^\varepsilon := R_\varepsilon \mathbf{e}[z, p] \quad \text{for } z \in \Omega \quad \text{and} \quad \varepsilon > 0.$$

Then the limit $\lim_{\varepsilon \rightarrow 0} |w_{g_z^\varepsilon}(z)|$ exists if and only if $z \in D$. For some $\alpha \in (0, 1)$ independent of z and p ,

$$\alpha \|s_z\|_Y^2 \leq \lim_{\varepsilon \rightarrow 0} |w_{g_z^\varepsilon}(z)| \leq \|s_z\|_Y^2,$$

where $s_z \in Y$ is the unique solution to $(F^*F)^{1/4}s_z = \mathbf{e}[z, p]$ in Y_0 . If $z \notin D$, then $|w_{g_z^\varepsilon}(z)|$ tends to infinity as $\varepsilon \rightarrow 0$ for any $p \in \mathbb{S}^{\ell-1}$.

Proof. The function g_z^ε can be explicitly computed as

$$g_z^\varepsilon = R_\varepsilon \mathbf{e}[z, p] = \sum_{j \in \mathbb{N}} f_\varepsilon(|\lambda_j|^2) \bar{\lambda}_j \langle \mathbf{e}[z, p], \psi_j \rangle_Y \psi_j \quad (26)$$

and $\|g_z^\varepsilon\|_Y^2 = \sum_{j \in \mathbb{N}} |f_\varepsilon(|\lambda_j|^2) \bar{\lambda}_j|^2 |\langle \mathbf{e}[z, p], \psi_j \rangle_Y|^2$ since ψ_j is an orthonormal family in Y .

Note that the restriction of the Herglotz wave function $w_{g_z^\varepsilon}(x)$ to D equals $p \cdot Hg_z^\varepsilon = \langle g_z^\varepsilon, \mathbf{e}[x, p] \rangle_Y$. The latter is, for fixed $z \in \Omega$, by Assumption 4(C) a bounded linear form on Y_0 . We can hence interchange this bounded linear form and the series in j ,

$$\begin{aligned} w_{g_z^\varepsilon}(x) &= p \cdot Hg_z^\varepsilon(x) = \sum_{j \in \mathbb{N}} f_\varepsilon(|\lambda_j|^2) \bar{\lambda}_j \langle \mathbf{e}[z, p], \psi_j \rangle_Y p \cdot H\psi_j(x) \\ &= \sum_{j \in \mathbb{N}} f_\varepsilon(|\lambda_j|^2) \bar{\lambda}_j \langle \mathbf{e}[z, p], \psi_j \rangle_Y \langle \psi_j, \mathbf{e}[x, p] \rangle_Y \\ &= \sum_{j \in \mathbb{N}} f_\varepsilon(|\lambda_j|^2) \bar{\lambda}_j \langle \mathbf{e}[z, p], \psi_j \rangle_Y \overline{\langle \mathbf{e}[x, p], \psi_j \rangle_Y}, \quad x \in D. \end{aligned}$$

Choosing $x = z$ shows that

$$w_{g_z^\varepsilon}(z) = \sum_{j \in \mathbb{N}} f_\varepsilon(|\lambda_j|^2) \bar{\lambda}_j |\langle \mathbf{e}[z, p], \psi_j \rangle_Y|^2, \quad z \in D. \quad (27)$$

If $z \in D$, then there exists by Assumption 4(D) a (unique) solution $s_z \in Y_0$ to the equation $(F^*F)^{1/4}s_z = \mathbf{e}[z, p]$. Note that

$$s_z = \sum_{j \in \mathbb{N}} \frac{\langle \mathbf{e}[z, p], \psi_j \rangle_Y}{|\lambda_j|^{1/2}} \psi_j, \quad \|s_z\|_Y^2 = \sum_{j \in \mathbb{N}} \frac{|\langle \mathbf{e}[z, p], \psi_j \rangle_Y|^2}{|\lambda_j|}, \quad (28)$$

and that the latter norm is finite if and only if $z \in D$ due to Assumption 4(A) and (D) and the well-known Picard criterion. Further,

$$\langle \mathbf{e}[z, p], \psi_j \rangle_Y = \langle (F^*F)^{1/4}s_z, \psi_j \rangle_Y = \langle s_z, (F^*F)^{1/4}\psi_j \rangle_Y = |\lambda_j|^{1/2} \langle s_z, \psi_j \rangle_Y.$$

Hence,

$$w_{g_z^\varepsilon}(z) = \sum_{j \in \mathbb{N}} f_\varepsilon(|\lambda_j|^2) |\lambda_j| \bar{\lambda}_j |\langle s_z, \psi_j \rangle_Y|^2, \quad z \in D.$$

Note that

$$|w_{g_z^\varepsilon}(z)| \leq \sum_{j \in \mathbb{N}} |f_\varepsilon(|\lambda_j|^2)| |\lambda_j|^2 |\langle s_z, \psi_j \rangle_Y|^2 \stackrel{(23)}{\leq} C \sum_{j \in \mathbb{N}} |\langle s_z, \psi_j \rangle_Y|^2 \leq C \|s_z\|_Y^2, \quad z \in D,$$

where the constant C from (23) is independent of ε . Hence, we can apply the theorem on dominated convergence to deduce that

$$\lim_{\varepsilon \rightarrow 0} w_{g_z^\varepsilon}(z) = \sum_{j \in \mathbb{N}} \left[\lim_{\varepsilon \rightarrow 0} f_\varepsilon(|\lambda_j|^2) \right] |\lambda_j| \overline{\lambda_j} |\langle s_z, \psi_j \rangle_Y|^2 = \sum_{j \in \mathbb{N}} \frac{\overline{\lambda_j}}{|\lambda_j|} |\langle s_z, \psi_j \rangle_Y|^2, \quad z \in D.$$

The absolute value of $\lim_{\varepsilon \rightarrow 0} w_{g_z^\varepsilon}(z)$ is hence bounded from above by

$$\lim_{\varepsilon \rightarrow 0} |w_{g_z^\varepsilon}(z)| \leq \sum_{j \in \mathbb{N}} |\langle s_z, \psi_j \rangle_Y|^2 = \|s_z\|_Y^2, \quad z \in D.$$

Moreover, by Assumption 4(C), $\lambda_j/|\lambda_j| = \exp(i\delta_j)$ with a phase δ_j contained in an interval J of length strictly smaller than π . Choose $\eta \in \mathbb{R}$ such that the shifted interval $J + \eta$ is centered at $\pi/2$, that is, $\text{dist}(J + \eta, 0) = \text{dist}(J + \eta, \pi) =: \delta > 0$. Since $|\exp(i\eta)| = 1$, we can write

$$\lim_{\varepsilon \rightarrow 0} |w_{g_z^\varepsilon}(z)| = \left| \sum_{j \in \mathbb{N}} e^{i\delta_j} |\langle s_z, \psi_j \rangle_Y|^2 \right| = \left| \sum_{j \in \mathbb{N}} e^{i(\delta_j + \eta)} |\langle s_z, \psi_j \rangle_Y|^2 \right|. \quad (29)$$

This choice of η implies that $\text{Im} \exp(i(\delta_j + \eta)) \geq \sin(\delta) =: \alpha > 0$ and hence

$$\lim_{\varepsilon \rightarrow 0} |w_{g_z^\varepsilon}(z)| \geq \lim_{\varepsilon \rightarrow 0} |\text{Im} w_{g_z^\varepsilon}(z)| \geq \sum_{j \in \mathbb{N}} \text{Im} e^{i(\delta_j + \eta)} |\langle s_z, \psi_j \rangle_Y|^2 \geq \alpha \|s_z\|_Y^2.$$

Let now $z \notin D$. Since the filter function f_ε is for fixed $\varepsilon > 0$ a bounded, real-valued function, the value of $w_{g_z^\varepsilon}(z)$ is bounded and its absolute value can be estimated from below using (27) by

$$\begin{aligned} |w_{g_z^\varepsilon}(z)| &= |e^{-i\eta} w_{g_z^\varepsilon}(z)| = |e^{i\eta} \overline{w_{g_z^\varepsilon}(z)}| \geq \text{Im} \left(e^{i\eta} \overline{w_{g_z^\varepsilon}(z)} \right) \\ &= \sum_{j \in \mathbb{N}} f_\varepsilon(|\lambda_j|^2) \text{Im} [e^{i\eta} \lambda_j] |\langle \mathbf{e}[z, p], \psi_j \rangle_Y|^2 \\ &= \sum_{j \in \mathbb{N}} f_\varepsilon(|\lambda_j|^2) |\lambda_j| \text{Im} [e^{i(\delta_j + \eta)}] |\langle \mathbf{e}[z, p], \psi_j \rangle_Y|^2 \end{aligned}$$

since, by definition, $\lambda_j/|\lambda_j| = \exp(i\delta_j)$. Estimating again $\text{Im} [\exp(i(\delta_j + \eta))] \geq \sin(\delta) = \alpha$, we obtain, for any $\varepsilon > 0$ and any $N_0 \in \mathbb{N}$,

$$|w_{g_z^\varepsilon}(z)| \geq \alpha \sum_{j=1}^{N_0} f_\varepsilon(|\lambda_j|^2) |\lambda_j| |\langle \mathbf{e}[z, p], \psi_j \rangle_Y|^2.$$

As $f_\varepsilon(|\lambda_j|^2) |\lambda_j| \rightarrow |\lambda_j|^{-1}$ for $\varepsilon \rightarrow 0$, taking the limit of the finite sum yields that

$$\lim_{\varepsilon \rightarrow 0} |w_{g_z^\varepsilon}(z)| \geq \alpha \sum_{j=1}^{N_0} \frac{|\langle \mathbf{e}[z, p], \psi_j \rangle_Y|^2}{|\lambda_j|} \quad \text{for arbitrary } N_0 \in \mathbb{N}.$$

However, since z does by assumption not belong to D , the function $\mathbf{e}[z, p]$ does by Assumption 4(D) not belong to the range of $(F^*F)^{1/4}$, i.e., the series $N_0 \mapsto \sum_{j=1}^{N_0} |\langle \mathbf{e}[z, p], \psi_j \rangle_Y|^2 / |\lambda_j|$ grows monotonically without finite upper bound as $N_0 \rightarrow \infty$. In consequence, for any positive zero sequence $\{\varepsilon_n\}_{n \in \mathbb{N}}$, the sequence $|w_{g_z^{\varepsilon_n}}(z)|$ cannot possess any finite accumulation point, that is, $|w_{g_z^\varepsilon}(z)|$ tends to infinity as $\varepsilon \rightarrow 0$. \square

Note that the last proof also shows that for fixed $\varepsilon > 0$ and $z \in \mathbb{R}^3$ it holds that

$$\begin{aligned} \alpha \sum_{j \in \mathbb{N}} f_\varepsilon(|\lambda_j|^2) |\lambda_j|^2 \frac{|\langle \mathbf{e}[z, p], \psi_j \rangle_Y|^2}{|\lambda_j|} &\leq |w_{g_\varepsilon}(z)| \leq \sum_{j \in \mathbb{N}} f_\varepsilon(|\lambda_j|^2) |\lambda_j|^2 \frac{|\langle \mathbf{e}[z, p], \psi_j \rangle_Y|^2}{|\lambda_j|} \\ &\leq C \sum_{j \in \mathbb{N}} \frac{|\langle \mathbf{e}[z, p], \psi_j \rangle_Y|^2}{|\lambda_j|} \end{aligned}$$

where the constants α and C are independent of ε and z .

4 Noisy Data and Regularization

In the context of the Linear Sampling method, considering noisy data means considering a perturbed far field operator. Two fundamental problems arise: Firstly, a perturbed far field operator may fail to be normal and thus the existence of an eigensystem is no longer assured. This means that $w_{g_\varepsilon}(z)$ as expressed in (27) will not be computable. Secondly, multiplicity of eigenvalues becomes an issue.

The first problem can be overcome by considering a singular system of F instead of an eigensystem. Define $\mu_j = |\lambda_j|$ and $\varphi_j = (1/\mu_j) F^* \psi_j$. Then $(\mu_j, \varphi_j, \psi_j)$ is a singular system of F ,

$$Fg = \sum_{j \in \mathbb{N}} \mu_j \langle g, \varphi_j \rangle_Y \psi_j, \quad g \in Y,$$

with orthonormal bases (φ_j) , (ψ_j) and the monotonically decreasing sequence of singular values μ_j . Also, (μ_j^2, φ_j) is an eigensystem of F^*F . Using the singular system, we compute

$$\begin{aligned} h_\varepsilon(z) &= w_{g_\varepsilon}(z) = \sum_{j \in \mathbb{N}} f_\varepsilon(|\lambda_j|^2) \bar{\lambda}_j |\langle \mathbf{e}[z, p], \psi_j \rangle_Y|^2 \\ &= \sum_{j \in \mathbb{N}} f_\varepsilon(|\lambda_j|^2) \langle \mathbf{e}[z, p], \psi_j \rangle_Y \langle \bar{\lambda}_j \psi_j, \mathbf{e}[z, p] \rangle_Y = \sum_{j \in \mathbb{N}} f_\varepsilon(\mu_j^2) \mu_j \langle \mathbf{e}[z, p], \psi_j \rangle_Y \langle \varphi_j, \mathbf{e}[z, p] \rangle_Y. \end{aligned} \quad (30)$$

To address the second problem, denote by $(\tilde{\mu}_m)$ the strictly monotonically decreasing sequence of distinct singular values of F and define m_j , $j \in \mathbb{N}$, such that $\tilde{\mu}_{m_j} = \mu_j$. Furthermore, we defined the spectral projections

$$P_m g = \sum_{j: m_j=m} \langle g, \varphi_j \rangle_Y \varphi_j, \quad m \in \mathbb{N}, \quad g \in Y.$$

For later use, we note that by orthogonality, we have

$$\|g\|^2 = \sum_{m \in \mathbb{N}} \|P_m g\|^2, \quad g \in Y. \quad (31)$$

Using the spectral projections, we further rewrite the indicator function as

$$\begin{aligned} h_\varepsilon(z) &= \sum_{j \in \mathbb{N}} f_\varepsilon(\mu_j^2) \mu_j \langle \mathbf{e}[z, p], \psi_j \rangle_Y \langle \varphi_j, \mathbf{e}[z, p] \rangle_Y = \sum_{j \in \mathbb{N}} f_\varepsilon(\mu_j^2) \langle F^* \mathbf{e}[z, p], \varphi_j \rangle_Y \langle \varphi_j, \mathbf{e}[z, p] \rangle_Y \\ &= \sum_{m \in \mathbb{N}} f_\varepsilon(\tilde{\mu}_m^2) \sum_{j: m_j=m} \sum_{\ell: m_\ell=m} \langle F^* \mathbf{e}[z, p], \varphi_j \rangle_Y \overline{\langle \mathbf{e}[z, p], \varphi_\ell \rangle_Y} \langle \varphi_j, \varphi_\ell \rangle_Y \\ &= \sum_{m \in \mathbb{N}} f_\varepsilon(\tilde{\mu}_m^2) \langle P_m F^* \mathbf{e}[z, p], P_m \mathbf{e}[z, p] \rangle_Y. \end{aligned} \quad (32)$$

We consider now a noisy far field operator F^δ such that $\|F - F^\delta\|_Y \leq \delta \leq \|F\|$ for some noise level $\delta \geq 0$. We then estimate

$$\|(F^\delta)^* F^\delta - F^* F\| \leq 3 \|F\| \delta.$$

The perturbed operator F^δ gives rise to a perturbed singular system $(\mu_j^\delta, \varphi_j^\delta, \psi_j^\delta)$ and associated projections P_m^δ which can be used to compute an approximation h_ε^δ of h_ε by the expression (30) or (32),

$$h_\varepsilon^\delta(z) = \sum_{j \in \mathbb{N}} f_\varepsilon(\mu_j^{\delta^2}) \mu_j^\delta \langle \mathbf{e}[z, p], \psi_j^\delta \rangle_Y \langle \varphi_j^\delta, \mathbf{e}[z, p] \rangle_Y \quad (33)$$

$$= \sum_{m \in \mathbb{N}} f_\varepsilon((\tilde{\mu}_m^\delta)^2) \langle P_m^\delta (F^\delta)^* \mathbf{e}[z, p], P_m^\delta \mathbf{e}[z, p] \rangle_Y. \quad (34)$$

In order to estimate the differences between the expressions for h_ε and h_ε^δ , we use two lemmas from perturbation theory for self-adjoint operators (see, e.g., Section IV-§3.1 and Section V-§4.3 in [18]).

Lemma 7. *Let A, B be bounded self-adjoint operators. Then $\text{dist}(\sigma(A), \sigma(B)) \leq \|A - B\|$, i.e.*

$$\sup_{\lambda \in \sigma(A)} \text{dist}(\lambda, \sigma(B)), \quad \sup_{\lambda \in \sigma(B)} \text{dist}(\lambda, \sigma(A)) \leq \|A - B\|.$$

Lemma 8. *Let A, B be bounded normal operators with monotonically decreasing sequences of distinct eigenvalues $\{\lambda_m^A\}_{m \in \mathbb{N}}, \{\lambda_m^B\}_{m \in \mathbb{N}}$. Denote by P_m^A and P_m^B the spectral projections of A and B , respectively. Assume that $\|A - B\| \leq \rho < d$ and that $\text{dist}(\lambda_m^A, \sigma(A) \setminus \{\lambda_m^A\}) = 2d$ for some $m \in \mathbb{N}$. If we further set*

$$\tilde{P}_m^B = \sum_{|\lambda_m^A - \lambda_\ell^B| < d} P_\ell^B \quad \text{then} \quad \|P_m^A - \tilde{P}_m^B\| \leq \frac{\rho}{d - \rho}.$$

In order to apply these lemmas for obtaining a regularization strategy, relatively large and well separated singular values of F need to be separated from the rest of the spectrum. We introduce a cut-off index

$$J(\delta) = \max \left\{ j : \text{dist}(\mu_j^2, \sigma(F^* F) \setminus \{\mu_j^2\}) > 2(3\|F\|\delta)^{1/3} \text{ and } m_j \leq \delta^{-1/6} \right\}.$$

We will also assume two bounds on the noise level δ : First, $\delta \leq (6\sqrt{2}\|F\|)^{-1}$, so that $(3\|F\|\delta)^{2/3} \leq 1/2$, and second $\delta < \max\{(\tilde{\mu}_1^2 - \tilde{\mu}_2^2)^3/(24\|F\|), 1\}$, so that $J(\delta) \geq 1$ (otherwise some of the sums below vanish). Since zero always belongs to the spectrum of the compact operator we note that the definition of $J(\delta)$ implies

$$2(3\|F\|\delta)^{1/3} < \mu_j^2 < \|F\|^2 \quad \text{for all } j = 1, \dots, J(\delta).$$

Obviously, $J(\delta) \rightarrow \infty$ as $\delta \rightarrow 0$.

To formulate a convergence theorem for a regularized version of the Linear Sampling method for noisy data, let us finally introduce a measure of the variation of the associated filter function,

$$\text{var}_{\delta'}(f_\varepsilon) = \sup \left\{ \left| f_\varepsilon(\lambda) - f_\varepsilon(\tilde{\lambda}) \right|, \quad 2\delta'^{1/3} \leq \lambda \leq \|F\|^2, \quad |\lambda - \tilde{\lambda}| \leq \delta' \right\}, \quad \delta' > 0.$$

Theorem 9. Suppose $\varepsilon(\delta)$, $0 < \delta \leq \max \{(6\sqrt{2}\|F\|)^{-1}, (\tilde{\mu}_1^2 - \tilde{\mu}_2^2)^3/(24\|F\|), 1\}$ satisfies

$$\|f_{\varepsilon(\delta)}\|_{\infty} |\mu_{J(\delta)}| \rightarrow 0, \quad \|f_{\varepsilon(\delta)}\|_{\infty} \sqrt{\delta} \rightarrow 0, \quad \text{var}_{3\|F\|\delta}(f_{\varepsilon(\delta)}) \rightarrow 0 \quad (\delta \rightarrow 0).$$

Then, for $z \in D$,

$$\lim_{\delta \rightarrow 0} h_{\varepsilon(\delta)}^{\delta}(z) = \lim_{\delta \rightarrow 0} w_{g_{\varepsilon(\delta)}}(z).$$

Proof. For $j \leq J(\delta)$, collect the eigenvalues of $(F^{\delta})^* F^{\delta}$ that are close enough to μ_j^2 so that the second lemma above can be applied with $d = (3\|F\|\delta)^{1/3} > \rho = 3\|F\|\delta$:

$$L(m) = \{\ell : |\tilde{\mu}_m^2 - (\tilde{\mu}_\ell^{\delta})^2| \leq 3\|F\|\delta\}, \quad m \leq m_{J(\delta)}.$$

Set

$$\tilde{J}(\delta) = \max\{\ell : \tilde{m}_\ell \in L(m) \text{ for some } m \leq m_{J(\delta)}\}.$$

With these definitions there holds

$$\left(\mu_{\tilde{J}(\delta)+1}^{\delta}\right)^2 \leq \mu_{J(\delta)}^2 - 3\|F\|\delta < \mu_{J(\delta)}^2. \quad (35)$$

Note also that $J(\cdot)$ is a strictly monotonically increasing function of δ .

We estimate from (30) and (33),

$$\begin{aligned} |h_{\varepsilon}(z) - h_{\varepsilon}^{\delta}(z)| &\leq \left| \sum_{j=1}^{J(\delta)} f_{\varepsilon}(\mu_j^2) \mu_j \langle \mathbf{e}[z, p], \psi_j \rangle_Y \langle \varphi_j, \mathbf{e}[z, p] \rangle_Y \right. \\ &\quad \left. - \sum_{j=1}^{\tilde{J}(\delta)} f_{\varepsilon}((\mu_j^{\delta})^2) \mu_j^{\delta} \langle \mathbf{e}[z, p], \psi_j^{\delta} \rangle_Y \langle \varphi_j^{\delta}, \mathbf{e}[z, p] \rangle_Y \right| \\ &+ \left| \sum_{j=J(\delta)+1}^{\infty} f_{\varepsilon}(\mu_j^2) \mu_j \langle \mathbf{e}[z, p], \psi_j \rangle_Y \langle \varphi_j, \mathbf{e}[z, p] \rangle_Y \right| \\ &+ \left| \sum_{j=\tilde{J}(\delta)+1}^{\infty} f_{\varepsilon}((\mu_j^{\delta})^2) \mu_j^{\delta} \langle \mathbf{e}[z, p], \psi_j^{\delta} \rangle_Y \langle \varphi_j^{\delta}, \mathbf{e}[z, p] \rangle_Y \right|. \end{aligned}$$

The two series are easily treated. The first can be estimated by

$$\begin{aligned} &\left| \sum_{j=J(\delta)+1}^{\infty} f_{\varepsilon}(\mu_j^2) \mu_j \langle \mathbf{e}[z, p], \psi_j \rangle_Y \langle \varphi_j, \mathbf{e}[z, p] \rangle_Y \right| \\ &\leq \|f_{\varepsilon}\|_{\infty} |\mu_{J(\delta)+1}| \sum_{j=J(\delta)+1}^{\infty} |\langle \mathbf{e}[z, p], \psi_j \rangle_Y \langle \varphi_j, \mathbf{e}[z, p] \rangle_Y| \leq \|f_{\varepsilon}\|_{\infty} |\mu_{J(\delta)}| \|\mathbf{e}[z, p]\|_Y^2 \quad (36) \end{aligned}$$

Similarly, we obtain, using (35),

$$\left| \sum_{j=\tilde{J}(\delta)+1}^{\infty} f_{\varepsilon}((\mu_j^{\delta})^2) \mu_j^{\delta} \langle \mathbf{e}[z, p], \psi_j^{\delta} \rangle_Y \langle \varphi_j^{\delta}, \mathbf{e}[z, p] \rangle_Y \right| \leq \|f_{\varepsilon}\|_{\infty} |\mu_{J(\delta)}| \|\mathbf{e}[z, p]\|_Y^2. \quad (37)$$

Using the representations (32) and (34), the remaining sum is split again into two parts,

$$\begin{aligned}
& \left| \sum_{j=1}^{J(\delta)} f_\varepsilon(\mu_j^2) \mu_j \langle \mathbf{e}[z, p], \psi_j \rangle_Y \langle \varphi_j, \mathbf{e}[z, p] \rangle_Y - \sum_{j=1}^{\tilde{J}(\delta)} f_\varepsilon((\mu_j^\delta)^2) \mu_j^\delta \langle \mathbf{e}[z, p], \psi_j^\delta \rangle_Y \langle \varphi_j^\delta, \mathbf{e}[z, p] \rangle_Y \right| \\
&= \left[\sum_{m=1}^{m_{J(\delta)}} \left[f_\varepsilon(\tilde{\mu}_m^2) \langle P_m F^* \mathbf{e}[z, p], P_m \mathbf{e}[z, p] \rangle_Y - \sum_{\ell \in L(m)} f_\varepsilon((\tilde{\mu}_\ell^\delta)^2) \langle P_\ell^\delta (F^\delta)^* \mathbf{e}[z, p], P_\ell^\delta \mathbf{e}[z, p] \rangle_Y \right] \right] \\
&\leq \sum_{m=1}^{m_{J(\delta)}} |f_\varepsilon(\tilde{\mu}_m^2)| \left| \langle P_m F^* \mathbf{e}[z, p], P_m \mathbf{e}[z, p] \rangle_Y - \sum_{\ell \in L(m)} \langle P_\ell^\delta (F^\delta)^* \mathbf{e}[z, p], P_\ell^\delta \mathbf{e}[z, p] \rangle_Y \right| \\
&\quad + \sum_{m=1}^{m_{J(\delta)}} \sum_{\ell \in L(m)} \left| f_\varepsilon(\tilde{\mu}_m^2) - f_\varepsilon((\tilde{\mu}_\ell^\delta)^2) \right| \left| \langle P_\ell^\delta (F^\delta)^* \mathbf{e}[z, p], P_\ell^\delta \mathbf{e}[z, p] \rangle_Y \right|.
\end{aligned}$$

Using the definition of $L(m)$, the second sum is seen to be bounded by

$$\begin{aligned}
& \sum_{m=1}^{m_{J(\delta)}} \sum_{\ell \in L(m)} \left| f_\varepsilon(\tilde{\mu}_m^2) - f_\varepsilon((\tilde{\mu}_\ell^\delta)^2) \right| \left| \langle P_\ell^\delta (F^\delta)^* \mathbf{e}[z, p], P_\ell^\delta \mathbf{e}[z, p] \rangle_Y \right| \\
&\leq \text{var}_{3\|F\|\delta}(f_{\varepsilon(\delta)}) \sum_{m=1}^{m_{J(\delta)}} \sum_{\ell \in L(m)} \left| \langle P_\ell^\delta (F^\delta)^* \mathbf{e}[z, p], P_\ell^\delta \mathbf{e}[z, p] \rangle_Y \right| \\
&\leq \text{var}_{3\|F\|\delta}(f_{\varepsilon(\delta)}) \|(F^\delta)^* \mathbf{e}[z, p]\|_Y \|\mathbf{e}[z, p]\|_Y \leq 2 \text{var}_{3\|F\|\delta}(f_{\varepsilon(\delta)}) \|F\| \|\mathbf{e}[z, p]\|_Y^2. \quad (38)
\end{aligned}$$

For the first sum, note first that because of orthogonality we have

$$\sum_{\ell \in L(m)} \langle P_\ell^\delta (F^\delta)^* \mathbf{e}[z, p], P_\ell^\delta \mathbf{e}[z, p] \rangle_Y = \sum_{\ell, n \in L(m)} \langle P_\ell^\delta (F^\delta)^* \mathbf{e}[z, p], P_n^\delta \mathbf{e}[z, p] \rangle_Y.$$

This and Lemma 8 can be applied to obtain

$$\begin{aligned}
& \left| \langle P_m F^* \mathbf{e}[z, p], P_m \mathbf{e}[z, p] \rangle_Y - \sum_{\ell \in L(m)} \langle P_\ell^\delta (F^\delta)^* \mathbf{e}[z, p], P_\ell^\delta \mathbf{e}[z, p] \rangle_Y \right| \\
&\leq \left| \langle P_m F^* \mathbf{e}[z, p], P_m \mathbf{e}[z, p] - \sum_{\ell \in L(m)} P_\ell^\delta \mathbf{e}[z, p] \rangle_Y \right| \\
&\quad + \left| \langle P_m F^* \mathbf{e}[z, p] - \sum_{\ell \in L(m)} P_\ell^\delta (F^\delta)^* \mathbf{e}[z, p], \sum_{n \in L(m)} P_n^\delta \mathbf{e}[z, p] \rangle_Y \right| \\
&\leq \left(\|P_m F^* \mathbf{e}[z, p]\|_Y + \left\| \sum_{n \in L(m)} P_n^\delta \mathbf{e}[z, p] \right\|_Y \right) \frac{3\|F\|\delta}{(3\|F\|\delta)^{1/3} - 3\|F\|\delta}
\end{aligned}$$

Standard estimates give

$$\frac{3\|F\|\delta}{(3\|F\|\delta)^{1/3} - 3\|F\|\delta} = \frac{(3\|F\|\delta)^{2/3}}{1 - (3\|F\|\delta)^{2/3}} \leq \frac{(3\|F\|\delta)^{2/3}}{1 - \frac{1}{2}} = 2(3\|F\|\delta)^{2/3}.$$

Using the Cauchy-Schwarz inequality and (31), we also obtain

$$\sum_{m=1}^{m_{J(\delta)}} \|P_m F^* \mathbf{e}[z, p]\|_Y \leq m_{J(\delta)} \left(\sum_{m=1}^{m_{J(\delta)}} \|P_m F^* \mathbf{e}[z, p]\|_Y^2 \right)^{1/2} \leq \delta^{-1/6} \|F^* \mathbf{e}[z, p]\|_Y,$$

and the corresponding result for $\sum_{m=1}^{m_{J(\delta)}} \left\| \sum_{n \in L(m)} P_n^\delta \mathbf{e}[z, p] \right\|$. Thus, we can estimate

$$\begin{aligned} \sum_{m=1}^{m_{J(\delta)}} |f_\varepsilon(\tilde{\mu}_m^2)| \left| \langle P_m F^* \mathbf{e}[z, p], P_m \mathbf{e}[z, p] \rangle_Y - \sum_{\ell \in L(m)} \langle P_\ell^\delta (F^\delta)^* \mathbf{e}[z, p], P_\ell^\delta \mathbf{e}[z, p] \rangle_Y \right| \\ \leq 2(3\|F\|)^{2/3} (1 + \|F\|) \|\mathbf{e}[z, p]\|_Y^2 \|f_\varepsilon\|_\infty \sqrt{\delta}. \end{aligned} \quad (39)$$

Together, the bounds (36)–(39) imply the assertion. \square

Quite similar arguments also prove that the perturbed indicator function will not remain bounded for a point outside the scatterer.

Corollary 10. *Assume that $\delta, \varepsilon(\delta)$ satisfy the conditions of Theorem 9. Then for $z \notin D$, $h_{\varepsilon(\delta)}^\delta(z)$ will not remain bounded as $\delta \rightarrow 0$.*

Proof. For $K \in \mathbb{N}$, set

$$\begin{aligned} h_\varepsilon^K(z) &= \sum_{j=1}^K f_\varepsilon(\mu_j^2) \mu_j \langle \mathbf{e}[z, p], \psi_j \rangle_Y \langle \varphi_j, \mathbf{e}[z, p] \rangle_Y, \\ h_\varepsilon^{K, \delta}(z) &= \sum_{j=1}^K f_\varepsilon(\mu_j^{\delta^2}) \mu_j^\delta \langle \mathbf{e}[z, p], \psi_j^\delta \rangle_Y \langle \varphi_j^\delta, \mathbf{e}[z, p] \rangle_Y. \end{aligned}$$

Assume there is some constant $C > 0$ and some $\delta_0 > 0$ such that $|h_{\varepsilon(\delta)}^\delta(z)| \leq C$ for all $\delta \in (0, \delta_0)$. We estimate

$$|h_{\varepsilon(\delta)}(z)| \leq |h_{\varepsilon(\delta)}(z) - h_{\varepsilon(\delta)}^{J(\delta)}(z)| + |h_{\varepsilon(\delta)}^{J(\delta)}(z) - h_{\varepsilon(\delta)}^{\tilde{J}(\delta), \delta}(z)| + |h_{\varepsilon(\delta)}^{\tilde{J}(\delta), \delta}(z) - h_{\varepsilon(\delta)}^\delta(z)| + C.$$

However, the three differences can be bounded as in the proof of Theorem 9 using (36), (38) as well as (39) and (37), respectively. Thus, we conclude that $|h_{\varepsilon(\delta)}(z)| = |w_{g_z^{\varepsilon(\delta)}}(z)|$ remains bounded as $\delta \rightarrow 0$, in contradiction to Theorem 6. \square

Remark 11. (a) *For specific regularization strategies, the conditions on the behaviour $\varepsilon(\delta)$ given in Theorem 9 take on a more concrete form. Considering Tikhonov regularization as in (24), for example, we can write the first condition as $\mu_{J(\delta)}/\varepsilon(\delta) \rightarrow 0$ ($\delta \rightarrow 0$) whereas the second and third conditions both follow from $\delta^{1/2}/\varepsilon(\delta) \rightarrow 0$ ($\delta \rightarrow 0$). In the case of the spectral value cut-off as in (25), the first condition follows again from $\mu_{J(\delta)}/\varepsilon(\delta) \rightarrow 0$ ($\delta \rightarrow 0$) and the second from $\delta^{1/2}/\varepsilon(\delta) \rightarrow 0$ ($\delta \rightarrow 0$) whereas the third condition only requires $\delta/\varepsilon(\delta) \rightarrow 0$ ($\delta \rightarrow 0$).*

(b) *Note that the regularization scheme requires information about the singular values of F to determine the parameter choice $\varepsilon(\delta)$. Due to Lemma 7 we know that the Hausdorff distance of the singular values of the data F and F^δ is as small as $\|(F^\delta)^* F^\delta - F^* F\| \leq 2\delta \|F^\delta\| + \delta^2$. Hence, at least for small noise level δ , replacing the singular values of F by those of F^δ yields a sufficiently accurate approximation.*

5 Numerical Experiments

We illustrate the theoretical results with two examples for the electromagnetic inverse shape identification problem introduced in Section 2.2. To approximate the scattered electromagnetic wave H^s from (11) for an incident electromagnetic plane wave of the form (12) we rely on a volumetric integral equation method that governs the corresponding electric field E^s , presented in [13, eq. (9.7)], that features a weakly singular volume integral operator. This integral equation requires that the contrast $q = 1 - 1/\varepsilon_r$ belongs to $C^{1,\alpha}(\mathbb{R}^3)$. A trigonometric collocation discretization of this integral equation that is rapidly converging for smooth contrasts and particularly easy to implement has been introduced in [17]. Given a solution E^s to the integral equation, its far field pattern in direction \hat{x} is computed by integrating against the far field of an electromagnetic dipole (see [17, eq. (6)]) and the far field of the corresponding scattered magnetic field H^s equals the cross product of the electric far field pattern with \hat{x} (see [13, eq. (6.24)]).

Our simulations use a set of $N = 120$ incident and scattering directions $\{\theta_j\}_{j=1}^N \subset \mathbb{S}^2$ derived from a quadrangulation of the sphere that is presented in [7, II.2.3.2.1], together with two associated orthogonal polarizations $\{p_j^{(1)}, p_j^{(2)}\}_{j=1}^N \subset \mathbb{S}^2$, i.e., $p_j^{(1,2)} \cdot \theta_j = 0$. We use the above-mentioned collocation scheme to simulate magnetic far field patterns for incident plane waves of the form (12) at wave number $k = \pi$ (all computations are done on a Linux workstation with 8 CPU cores and 32 GB RAM). This yields a matrix \mathbb{F}_N of size $2N \times 2N$ containing approximations to the exact values of $H^\infty(\theta_i, \theta_j, p_j^{(1,2)})$ with a certain numerical error $\delta' > 0$. Using a constant interpolation projection onto the quadrangles one shows that this matrix is an interpolation discretization of an approximation to the far field operator F from (13) that converges in the operator norm, if the interpolation and the discretization error both tend to zero, see [22] for details. (This requires the number of directions N to tend to infinity.) The two dielectric scatterers we consider are a penetrable medium described by $\varepsilon_1(x) = 1 + \sin^2(\pi/2(1 - |x + (1, 1, 1)|)_+)$, see Figure 2(a), and $\varepsilon_2(x) = 1 + \sin^2(\pi/2(1 - |x + (1, 1, 1)|)_+) + \sin^2(\pi/2(1 - |x - (1, 1, 1)|)_+)$, see Figure 2(b). (The positive part $(a)_+$ is defined by $(a)_+ = \max(a, 0)$.) The polarization vector p used to construct the test functions $\mathbf{e}[z, p]$ equals $p = (1, 1, 1)^\top / \sqrt{3}$ in all examples (it has only a minor effect on the resulting images).

For this computational setting, the above-described far-field matrix \mathbb{F}_N possesses a normality error $\|\mathbb{F}_N^* \mathbb{F}_N - \mathbb{F}_N \mathbb{F}_N^*\|_2 / \|\mathbb{F}_N^* \mathbb{F}_N\|_2$ in the spectral matrix norm of 0.011 for ε_1 and 0.0133 for ε_2 , respectively. Since the synthetic scattering data contains noise we regularize all three methods (for the Factorization and Linear Sampling method, we choose the classical way of Tikhonov regularization described, e.g., in [9]). Using the singular value decomposition $(\mu_j, \varphi_j, \psi_j)_{j=1}^{2N}$ of \mathbb{F}_N we evaluate the testfunction $\mathbf{e}[z, p]$ at directions $\{\theta_j\}_{j=1}^N \subset \mathbb{S}^2$ used for the forward computations and project into the tangent space. This yields a vector $\mathbf{e}_N[z, p]$ of length 240 and allows to plot

$$z \mapsto \left(\sum_{j=1}^{2N} \frac{\mu_j}{(|\mu_j| + \varepsilon)^2} |\langle \mathbf{e}_N[z, p], \varphi_j \rangle_{\mathbb{C}^{2N}}|^2 \right)^{-1} \quad \text{for a regularization parameter } \varepsilon > 0,$$

For the Linear Sampling method we plot the reciprocal of the norm of the Tikhonov regularization $g_N = g_N(z, \varepsilon) \in \mathbb{C}^{2N}$, solution to the linear system

$$(\mathbb{F}_N^* \mathbb{F}_N + \varepsilon I_N) g_N = \mathbb{F}_N^* \mathbf{e}_N[z, p],$$

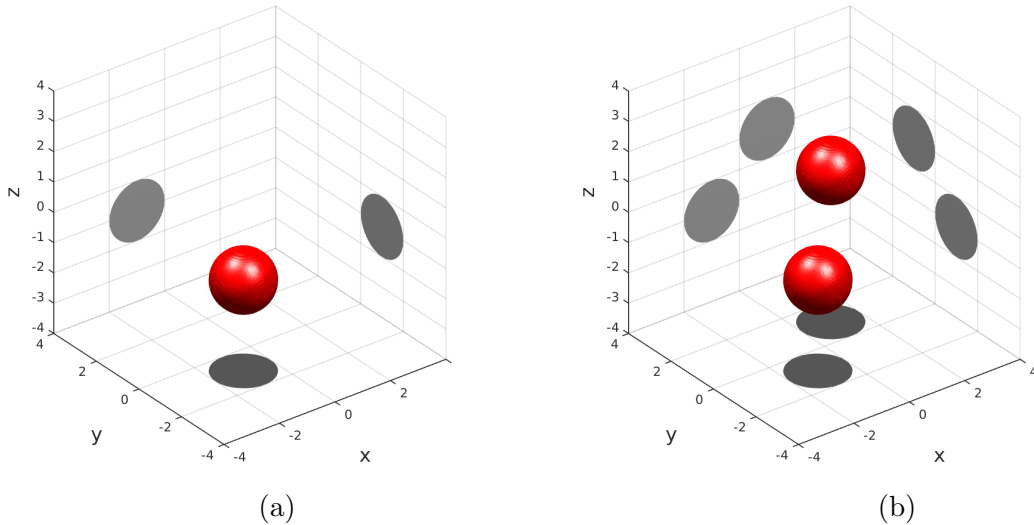


Figure 2: Contour plots of the two dielectric scatterers (a) ε_1 and (b) ε_2 .

as a function of z . The vector $g_N = g_N(z, \varepsilon)$ hence plays the role of the density g_z^ε in the above theoretic statements. To obtain an indicator function via the alternative formulation of the Linear Sampling method (compare Theorem 6) we evaluate a discretization of the Herglotz wave function $w_{g_z^\varepsilon}(z)$ following (26),

$$z \mapsto \frac{4\pi}{N} \sum_{j=1}^{2N} g_N(z, \varepsilon)(j) \overline{\mathbf{e}_N[z, p](j)}.$$

(Since the chosen directions correspond to a quadrangulation of \mathbb{S}^2 with quadrangles of equal area, no integration weights are necessary.)

In some experiments we perturb the simulated data \mathbb{F}_N by a random matrix with uniformly distributed entries in $[-a, a]$ such that the relative noise level after perturbation equals 0.05. Note that computing the parameter ε by a discrepancy principle pointwise for each z did not improve the image quality in our setting; we have hence chosen $\varepsilon = 0.02$ and $\varepsilon = 0.05$ independent of z and independent of the employed method in case that the artificial noise level equals 0% and 5%, respectively. All reconstructions of a scatterer at a fixed noise level are obtained from the same perturbed data and all are scaled to have maximum norm equal to one.

Figure 3 shows reconstructions for the dielectricity ε_1 , supported in the ball of radius one centered at $-(1, 1, 1)^\top$. (For each plot, an iso-surface is shown; the level $c > 0$ is always chosen such that the size of the reconstructed scatterer roughly equals the size of the support of the exact contrast.) When no artificial noise is added, all three methods provide a good estimate on the shape of the scatterer that remains stable up to a noise level of 5%.

Figure 4 shows reconstructions for the dielectric medium from Figure 2(b) that is supported on two balls of radius one centered at $\pm(1, 1, 1)^\top$. The quality of the results are quite similar to those obtained in Figure 3 and the same remarks apply.

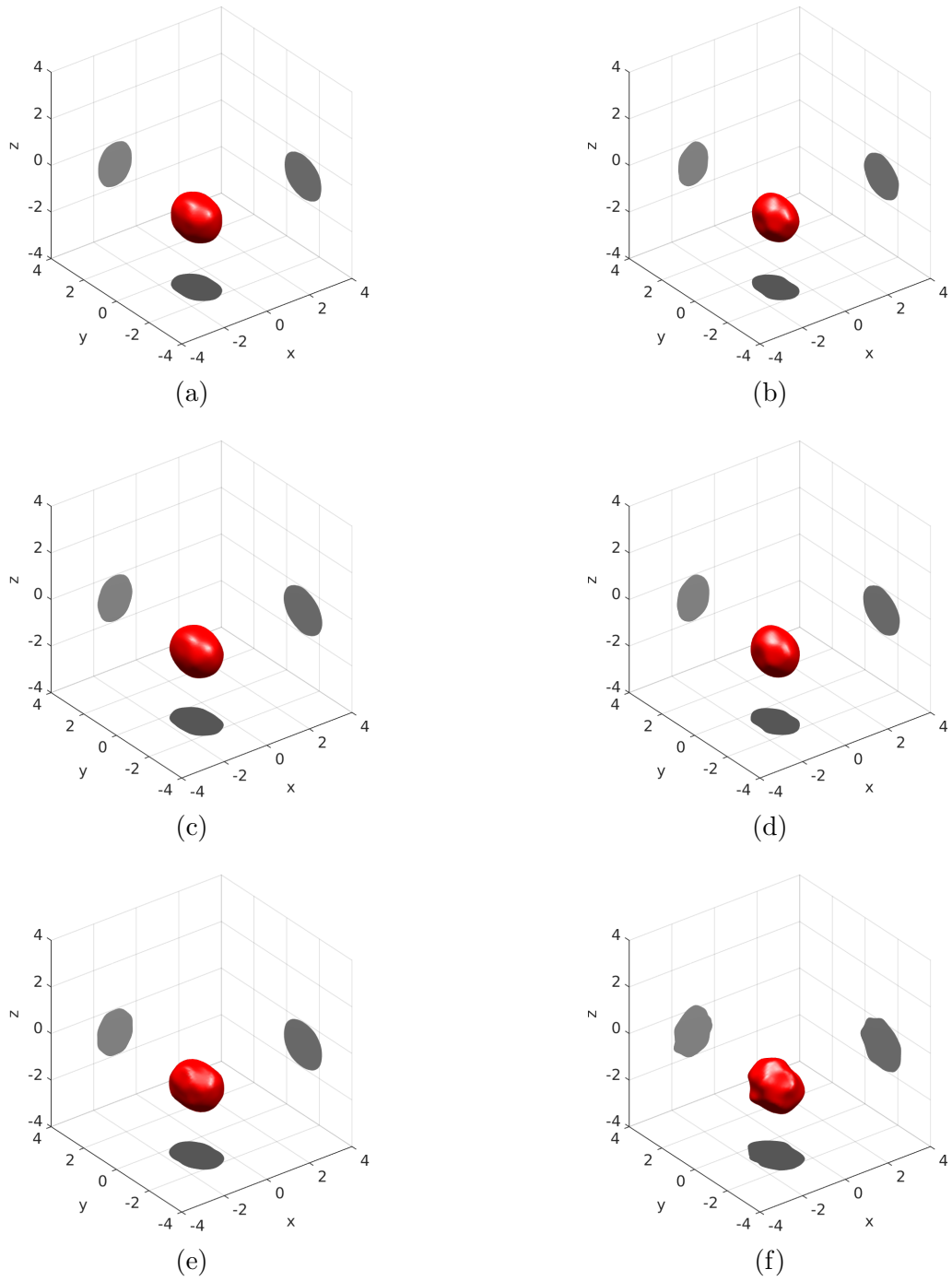


Figure 3: Reconstructions of the dielectric medium ε_1 , see Figure 2(a). Right column (a,c,e) no artificial noise. Left column (b,d,f) 5% artificial noise. (a,b) Factorization method. (c,d) Linear Sampling method. (e,f) Alternative Linear Sampling method.

Acknowledgements

The research of AL was partly supported through an exploratory project granted by the University of Bremen in the framework of its institutional strategy, funded by the excellence initiative

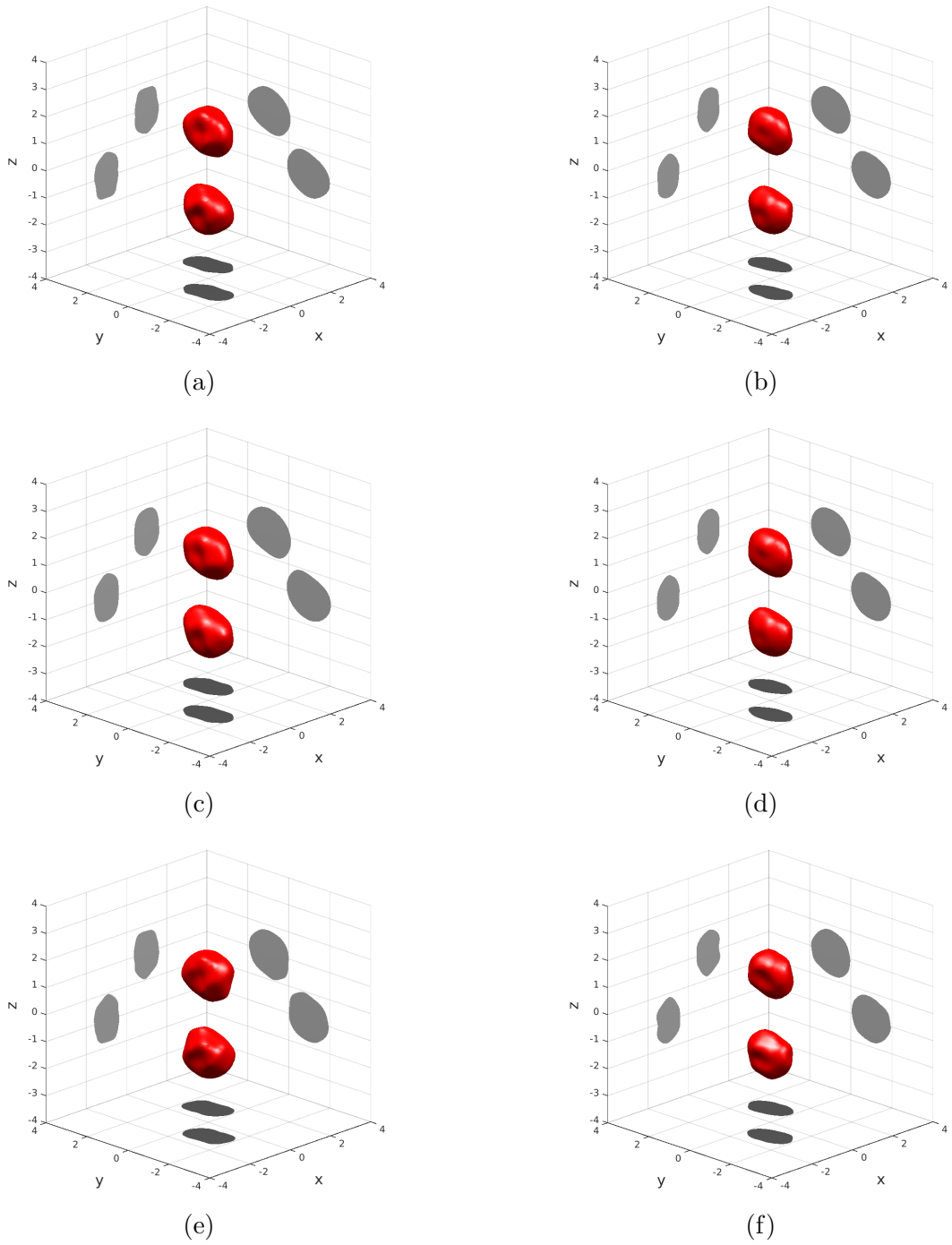


Figure 4: Reconstructions of the dielectric medium ε_2 , see Figure 2(b). Right column (a,c,e) no artificial noise. Left column (b,d,f) 5% artificial noise. (a,b) Factorization method. (c,d) Linear Sampling method. (e,f) Alternative Linear Sampling method.

of the federal and state governments of Germany.

References

- [1] R. Aramini, G. Caviglia, A. Massa, and M. Piana. The linear sampling method and energy conservation. *Inverse Probl.*, 26(5):055004, 2010.
- [2] T. Arens. Linear sampling methods for 2D inverse elastic wave scattering. *Inverse Problems*, 17:1445–1464, 2001.
- [3] T. Arens. Why linear sampling works. *Inverse Problems*, 20:163–173, 2004.
- [4] T. Arens and A. Lechleiter. The linear sampling method revisited. *J. Int. Eq. Appl.*, 21:179–202, 2009.
- [5] F. Cakoni and D. Colton. *Qualitative Methods in Inverse Scattering Theory. An Introduction*. Springer, Berlin, 2006.
- [6] F. Cakoni, D. Colton, and P. Monk. *The linear sampling method in inverse electromagnetic scattering*. Volume 80 of CBMS-NSG Regional Conference Series in Applied Mathematics. SIAM, 2011.
- [7] O. Cessenat. *Application d’une nouvelle formulation variationnelle aux équations d’ondes harmoniques. Problèmes de Helmholtz et de Maxwell*. PhD thesis, Université Paris IX Dauphine, 1996.
- [8] J. Choi and S. Kim. Neumann functions for second order elliptic systems with measurable coefficients. *Trans. Amer. Math. Soc.*, 2013.
- [9] D. Colton, J. Coyle, and P. Monk. Recent developments in inverse acoustic scattering theory. *SIAM Review*, 42:396–414, 2000.
- [10] D. Colton and A. Kirsch. A simple method for solving inverse scattering problems in the resonance region. *Inverse Problems*, 12:383–393, 1996.
- [11] D. Colton and R. Kress. Eigenvalues of the far field operator for the Helmholtz equation in an absorbing medium. *SIAM J. Appl. Math.*, 55:1724–1735, 1995.
- [12] D. Colton, M. Piana, and R. Potthast. A simple method using Morozov’s discrepancy principle for solving inverse scattering problems. *Inverse Problems*, 13:1477–1493, 1997.
- [13] D. L. Colton and R. Kress. *Inverse acoustic and electromagnetic scattering theory*. Springer, 3rd edition, 2013.
- [14] B. Gebauer, M. Hanke, A. Kirsch, W. Muniz, and C. Schneider. A sampling method for detecting buried objects using electromagnetic scattering. *Inverse Problems*, 21:2035–2050, 2005.
- [15] B. Gebauer, M. Hanke, and C. Schneider. Sampling methods for low-frequency electromagnetic imaging. *Inverse Problems*, 24:015007, 2008.
- [16] M. Hanke. Why linear sampling really seems to work. *Inverse Probl. Imaging*, 2:373–395, 2008.

- [17] T. Hohage. Fast numerical solution of the electromagnetic medium scattering problem and applications to the inverse problem. *J. Comp. Phys.*, 214:224–238, 2006.
- [18] T. Kato. *Perturbation theory for linear operators*. Springer, repr. of the 1980 edition, 1995.
- [19] A. Kirsch. Characterization of the shape of a scattering obstacle using the spectral data of the far field operator. *Inverse Problems*, 14:1489–1512, 1998.
- [20] A. Kirsch. *An introduction to the mathematical theory of inverse problems*. Springer, 2nd edition, 2011.
- [21] A. Kirsch and N. I. Grinberg. *The Factorization Method for Inverse Problems*. Oxford Lecture Series in Mathematics and its Applications 36. Oxford University Press, 2008.
- [22] A. Lechleiter and Z. Jiang. Stable computation of interior eigenvalues from far field data. *Preprint, available on demand*, 2014.
- [23] A. Lechleiter and T. Rienmüller. Factorization method for the inverse Stokes problem. *Inverse Problems and Imaging*, 7:1271–1293, 2013.
- [24] W. McLean. *Strongly Elliptic Systems and Boundary Integral Operators*. Cambridge University Press, Cambridge, UK, 2000.
- [25] C. Miranda. *Partial differential equations of elliptic type*. Springer, 2., rev. edition, 1970.
- [26] J.-C. Nédélec. *Acoustic and Electromagnetic Equations*. Springer, New York, 2001.